

# Spectropolarimetry of the massive post-red supergiants IRC +10420 and HD 179821

M. Patel,<sup>1,2\*</sup> R. D. Oudmaijer,<sup>1</sup> J. S. Vink,<sup>3,4</sup> J. E. Bjorkman,<sup>5</sup> B. Davies,<sup>1,6</sup>  
M. A. T. Groenewegen,<sup>7</sup> A. S. Miroshnichenko<sup>8</sup> and J. C. Mottram<sup>1</sup>

<sup>1</sup>*School of Physics and Astronomy, University of Leeds, Woodhouse Lane, Leeds LS2 9JT*

<sup>2</sup>*Astrophysics Group, Imperial College London, Blackett Laboratory, Prince Consort Road, London SW7 2AZ*

<sup>3</sup>*Armagh Observatory, College Hill, Armagh BT61 9DG*

<sup>4</sup>*Lennard–Jones Laboratory, Astrophysics, Keele University, Keele ST5 5BG*

<sup>5</sup>*Ritter Observatory, M.S. 113, Department of Physics and Astronomy, University of Toledo, Toledo, OH 43606-3390, USA*

<sup>6</sup>*Chester F. Carlson Centre for Imaging Science, Rochester Institute of Technology, 54 Lomb Memorial Drive, Rochester, NY 14623-5604, USA*

<sup>7</sup>*Instituut voor Sterrenkunde, K.U. Leuven, Celestijnenlaan 200 D, 3001 Leuven, Belgium*

<sup>8</sup>*Department of Physics and Astronomy, University of North Carolina at Greensboro, PO Box 26170, Greensboro NC 27402-6170, USA*

Accepted 2007 December 21. Received 2007 December 20; in original form 2007 August 3

## ABSTRACT

We present medium resolution spectropolarimetry and long-term photo-polarimetry of two massive post-red supergiants, IRC +10 420 and HD 179 821. The data provide new information on their circumstellar material as well as their evolution. In IRC +10 420, the polarization of the H $\alpha$  line is different to that of the continuum, which indicates that the electron-scattering region is not spherically symmetric. The observed long-term changes in the polarimetry can be associated with an axisymmetric structure, along the short axis of the extended reflection nebulosity. Long-term photometry reveals that the star increased in temperature until the mid-nineties, after which the photospheric flux in the optical levelled off. As the photometric changes are mostly probed in the red, they do not trace high stellar temperatures sensitively. So, it is not obvious whether the star has halted its increase in temperature or not. For HD 179 821, we find no polarization effects across any absorption or emission lines, but observe very large polarization changes of the order of 5 per cent over 15 yr. During the same period, the optical photometry displayed modest variability at the 0.2 mag level. This is unexpected, because large polarization changes are generally accompanied by strong photometric changes. Several explanations for this puzzling fact are discussed. Most of which, involving asymmetries in the circumstellar material, seem to fail as there is no evidence for the presence of hot, dusty material close to the star. A caveat is that the sparsely available near-infrared photometry could have missed periods of strong polarization activity. The variations may be explained by the presence of a non-radially pulsating photosphere. Changes in the photometry hint at an increase in temperature corresponding to a change through two spectral subclasses over the past 10 yr.

**Key words:** techniques: polarimetric – circumstellar matter – stars: evolution – stars: individual: IRC +10 420 – stars: individual: HD 179 821.

## 1 INTRODUCTION

Due to the steepness of the initial mass function, massive stars ( $\gtrsim 8 M_{\odot}$ ) are extremely rare. This is exacerbated by their comparatively short lifetimes. Yet, although rare, these objects have a crucial impact on the interstellar medium due to their strong winds

and high mass-loss rates, and can dominate the light output of entire galaxies.

An area of current interest is that massive evolved stars are often surrounded by bipolar nebulae (Weis 2003). Later in the evolution of a star, using spectropolarimetry, it is now established that the ejecta of supernovae (SN) deviate from spherical symmetry (e.g. Wang et al. 2003; Leonard et al. 2005). It is as yet unclear whether this is due to asymmetric explosions, axisymmetric stellar winds or a pre-existing density contrast in the surrounding material (e.g. Dwarkadas & Balick 1998; Dwarkadas & Owocki 2002). Wind

\*E-mail: m.patel06@imperial.ac.uk

axisymmetry may imply fast rotation, and be related to the beaming of SN explosions, which may be the origin of the extremely luminous, beamed gamma-ray bursts (e.g. Mazzali et al. 2003; Mészáros 2003).

Here, we address the issue by investigating the circumstellar ejecta of two yellow hypergiants, IRC +10420 and HD 179 821. These objects are thought to have evolved off the post-red supergiant branch and are still surrounded by mass ejected during a previous mass losing phase. Only a few yellow hypergiants are known (see the review by de Jager 1998), and the number of such hypergiants with circumstellar dust is even smaller – only IRC +10420 and HD 179 821 belong to this class (see e.g. Oudmaijer et al. 2008). Therefore, the study of these two unique objects is important in its own right.

As these stars are distant (3–5 kpc), the direct imaging of their innermost regions is currently beyond the reaches of current technology, although interferometry is starting to resolve the winds of evolved stars (de Wit et al. 2007). Observing with spectropolarimetry allows us to probe regions much closer to the star. Spectropolarimetry was first effectively used in the study of classical Be stars using the presence of ‘line effects’ (Poecckert 1975; Poecckert & Marlborough 1976). These are changes in polarization across spectral lines that have an emission component. They occur because emission-line photons arise over a larger volume than the stellar continuum photons. Consequently, the emission-line photons undergo fewer scatterings as they ‘see’ fewer electrons, resulting in a lower polarization than the continuum. We normally only observe a net polarization change if the geometry of the electron-scattering region is aspherical. Many authors have confirmed that this technique provides evidence that envelope geometries around Be stars are indeed disc-like (Dougherty & Taylor 1992; Quirrenbach et al. 1997; Wood, Bjorkman & Bjorkman 1997). More recently, the technique has been used to investigate the geometry of circumstellar material around Herbig Ae/Be stars. Studies by Oudmaijer & Drew (1999) and Vink et al. (2002) show that most Herbig stars exhibit line effects, indicating aspherical electron-scattering regions. For a recent review, see Oudmaijer (2007). With regard to evolved stars, Davies, Oudmaijer & Vink (2005) conducted a study of luminous blue variables (LBVs) using spectropolarimetry. They found that 50 per cent of the objects observed exhibited polarization changes across  $H\alpha$ , indicating that some asphericity lies at the base of the stellar wind. Furthermore, they found several objects for which the position angle varied randomly with time, leading them to conclude that the wind around these stars is clumpy (see also Nordsieck et al. 2001).

IRC +10420 is now well accepted as a massive, evolved object (e.g. Jones et al. 1993; Oudmaijer et al. 1996; Humphreys, Davidson & Smith 2002). This is mainly based on its large distance, high outflow velocity ( $40 \text{ km s}^{-1}$ ) and high luminosity implied from the hypergiant spectrum. The situation for HD 179 821 is less certain. The presence of non-radial pulsations coupled with comparatively modest photometric changes suggests a massive nature (Le Coroller et al. 2003). Furthermore, its circumstellar material has a large expansion velocity of  $30 \text{ km s}^{-1}$ , as measured in CO, suggesting the star is a supergiant (Kastner & Weintraub 1995). On the other hand, the overabundance of *s*-process elements and the low metallicity suggest HD 179 821 is perhaps a lower mass post-asymptotic giant branch (AGB) star (Zacs et al. 1996; Reddy & Hrivnak 1999; Thévenin, Parthasarathy & Jasniewicz 2000).

Although the latter’s nature is a bit more uncertain, there are some striking similarities between IRC +10420 and HD 179 821. When observed as part of a larger sample of post-AGB stars, these

two objects are often markedly different from the rest. In particular, their high outflow velocities (the average outflow velocity for post-AGB and AGB stars is  $15 \text{ km s}^{-1}$ ) require much higher luminosities if powered by radiation pressure alone (Habing, Tignon & Tielens 1994). They were the only objects that showed extensive reflection nebulae in a large survey by Kastner & Weintraub (1995). Jura, Velusamy & Werner (2001) point out the enormous difference between the space velocities of IRC +10420 and HD 179 821 when compared against low-mass post-AGB stars. Furthermore, both objects have an exceptionally strong O 17 774 triplet absorption feature indicating a high luminosity (Humphreys et al. 1973 and Reddy & Hrivnak 1999, based on Slowik & Peterson 1995). We therefore proceed with both objects and assume they are evolved post-red supergiants.

Recently, both objects have been observed at arcsec resolution in CO by Castro-Carrizo et al. (2007) who found, in accordance with previous estimates, that their mass-loss rates exceeded  $10^{-4} M_{\odot} \text{ yr}^{-1}$  when they were in the red supergiant phase. The envelopes show mild deviations from spherical symmetry in their data.

This paper is organized as follows. In Section 2, we review the experimental set-up and explain how the data have been reduced. We present our results for each object in Section 3, and use the new spectropolarimetric data together with past polarization measurements to investigate the nature of the circumstellar environments around each of the stars, which is discussed in Section 4. We conclude in Section 5.

## 2 OBSERVATIONS

We describe our most recent data in detail. Similar observations taken earlier are briefly discussed, with the relevant differences highlighted. The linear spectropolarimetric data were taken on the night of 2004 September 30 using the Intermediate Dispersion Spectrograph and Imaging System (ISIS) spectrograph on the 4.2-m William Herschel Telescope (WHT), La Palma. A MARCONI2 CCD detector with a R1200R grating was used. This yielded a spectral coverage of 6150–6815 Å and gave a spectral resolution of  $34 \text{ km s}^{-1}$  at  $H\alpha$ . The seeing was about 2 arcsec, and a slit with a width of 1 arcsec was used. The linear polarimetric component of the data was analysed using the polarization optics equipment present on the ISIS spectrograph. The object and the sky background were simultaneously observed using additional holes in the dekker mask. A calcite block was then used to split the rays into two perpendicularly polarized beams (the o and e rays). A complete data set therefore consists of four spectra observed at  $0^{\circ}$  and  $45^{\circ}$  (to measure Stokes  $Q$ ) and  $22.5^{\circ}$  and  $67.5^{\circ}$  (to measure Stokes  $U$ ).

All data reduction steps used the FIGARO software maintained by Starlink and included bias subtraction, cosmic ray removal, bad pixel correction, spectrum straightening and flat-fielding. Wavelength calibration was carried out using observations of a Copper–Argon lamp taken throughout the run. The data were then imported into the package CCD2POL (also maintained by Starlink), to produce the Stokes  $Q$  and  $U$  parameters. The degree of polarization and its PA can then be found from

$$p^2 = Q^2 + U^2, \quad (1)$$

$$\theta = 0.5 \times \arctan \left( \frac{U}{Q} \right). \quad (2)$$

Finally, the data were position angle-calibrated using a set of polarization standard stars observed during the run.

**Table 1.** New polarimetric observations of HD 179 821 and IRC +10420 measured in the  $R$  band. For the spectropolarimetric data (those taken at the AAT and WHT), the polarization was measured in the continuum region close to  $H\alpha$ , while the final two columns are the polarizations at the line centres. The  $H\alpha$  line-centre polarization of HD 179 821 was not calculated as no line effect was observed, and therefore this measurement would be equal to the continuum polarization. The systematic error of the AAT and the WHT spectropolarimetric data is estimated to be of the order of 0.10 and 0.15 per cent, respectively.

Object	Telescope	Date	Julian date	per cent (P)	PA ( $^\circ$ )	per cent ( $H\alpha$ )	PA ( $H\alpha$ ) ( $^\circ$ )
HD 179 821	AAT	2002 September 15	2452533	$1.99 \pm 0.11$	$40 \pm 2$		
	WHT	2004 September 30	2453279	$2.00 \pm 0.15$	$36 \pm 3$		
IRC +10420	NOT	1998 January 16	2450830	$1.95 \pm 0.05$	$174 \pm 1$		
	NOT	1998 May 16	2450950	$1.80 \pm 0.03$	$174 \pm 1$		
	AAT	2002 September 18	2452536	$2.12 \pm 0.11$	$173 \pm 2$	$1.28 \pm 0.11$	$10 \pm 2$
	AAT	2003 August 15	2452867	$2.35 \pm 0.11$	$179 \pm 1$	$1.61 \pm 0.11$	$11 \pm 1$
	WHT	2004 September 30	2453279	$3.40 \pm 0.15$	$174 \pm 2$	$1.93 \pm 0.15$	$11 \pm 2$

Polarimetric data should only be limited by photon statistics. For example, we expect an error of about 0.1 per cent for a detection of  $10^6$  photons, and significantly smaller when large parts of the spectra are binned. However, the presence of systematic errors such as scattered light and instrumental polarization often outweigh these photon-noise errors, and we estimate the errors in the present data to be of the order of 0.15 per cent. The observations of two zero-polarization objects show that the instrumental polarization is less than 0.15 per cent. We have made no attempt to correct for either instrumental or interstellar polarization (ISP), as these only add a constant ( $Q$ ,  $U$ ) vector to the data and therefore will not affect whether we observe a line effect.

## 2.1 Additional Data

### 2.1.1 Spectropolarimetry

Further data of IRC +10420 and HD 179 821 was obtained during previous observing runs. Spectropolarimetric observations of IRC +10420 were obtained using the 3.9-m Anglo-Australian Telescope (AAT) on 2002 September 18 and 2003 August 15. HD 179 821 was observed on 2002 September 15 at the AAT. The 2002 data are taken with a lower spectral resolution (2.1 Å) and the 2003 data are taken at comparable resolution to the current WHT data. We refer to Davies et al. (2005) for more details on the observations taken at the AAT in 2002 and 2003.

### 2.1.2 Photometry and polarimetry

We also obtained additional photometric and polarimetric data of IRC +10420. Hitherto unpublished broad-band polarimetry was obtained in January and May 1998 using the 2.5-m Nordic Optical Telescope (NOT) in La Palma, and on one of these nights  $BVRI$  photometry were obtained. These observations are described in Oudmaijer et al. (2001). Johnson  $BVRIJHK$  observations were obtained in 1998 on the 1-m telescope at the Tien-Shan Astrophysical Observatory (TSAO) (Kazakhstan) with the 2D-channel photometer-polarimeter FP3U of the Pulkovo Observatory (Bergner et al. 1988). Further near-infrared (near-IR) photometry was obtained employing the 1.5-m Carlos Sánchez Telescope (CST) in Tenerife. Details of the observing procedures can be found in Kerschbaum, Groenewegen & Lazaro (2006). The results are presented in Tables 1 and 2.  $R$ -band polarimetric data and optical and near-IR photometric data taken from the literature, for both objects, are described in Tables 3 and 4, respectively.

## 3 RESULTS

### 3.1 IRC +10420

#### 3.1.1 Spectropolarimetry

In Fig. 1, we have plotted the polarimetric data around  $H\alpha$  taken in 2002, 2003 and 2004. These data show ‘triplots’ of the spectropolarimetry, along with graphs plotting the Stokes  $Q$ ,  $U$  vectors against each other.

IRC +10420 displays  $H\alpha$  emission with a total equivalent width (EW) of  $-50$  Å. The emission line is unresolved in the lower resolution 2002 data. The other, higher resolution, data indicate a

**Table 2.** Photometry of IRC +10420. The data come from the CST, the NOT and the TSAO (see the text for details). Typically, the photometric errors are of the order of 0.01–0.03 mag.

Julian date	Telescope	$B - V$	$V$	$V - R$	$R - I$	$J$	$H$	$K$
2450268	CST					5.62		
2450303	CST					5.36	4.40	3.45
2450643	CST					5.40	4.44	3.50
2450690	CST					5.40	4.45	3.49
2450707	CST					5.37	4.43	3.38
2450950	NOT	2.76	11.06	2.40	1.70			
2450985	CST					5.38	4.44	3.48
2451037	TSAO	2.58	11.12	2.42	1.60			
2451039	TSAO	2.67	11.11	2.41	1.58			
2451042	TSAO	2.58	11.13	2.42	1.54			
2451043	TSAO	2.73	11.06	2.49	1.61			
2451047	TSAO	2.51	11.01	2.41	1.58	5.63	4.55	3.73
2451048	TSAO	2.75	11.03	2.47	1.60	5.43	4.57	3.58
2451050	TSAO	2.67	11.01	2.46	1.66			
2451052	TSAO	2.75	11.03	2.47	1.59	5.35	4.44	3.53
2451057	TSAO	2.76	10.96	2.47	1.64			
2451063	TSAO	2.60	10.95	2.43	1.59			
2451075	TSAO	2.70	11.16	2.52	1.60			
2451082	TSAO	2.66	11.09	2.47	1.59			
2451083	TSAO	2.72	11.05	2.48	1.60			
2451087	CST					5.24	4.29	3.33
2451099	TSAO	2.62	11.16	2.56	1.66			
2451100	TSAO	2.71	11.16	2.54	1.66			
2451103	TSAO	2.76	11.13	2.51	1.54			
2451104	TSAO	2.72	11.03	2.48	1.59			
2451147	CST					5.35	4.42	3.46
2451245	TSAO					5.32	4.47	3.56
2451292	CST					5.40	4.45	3.57

**Table 3.** *R* band polarimetric observations of HD 179 821 and IRC +10 420 taken from the literature. The observational period is given in the second column. The last three columns show the number of observations taken, the literature source and the method. Although Craine et al. (1976) made several observations of IRC +10 420, these values were averaged to a single data point in our study. We measured the continuum close to H $\alpha$  from the spectropolarimetric data in order to facilitate comparison with the *R*-band data.

Object	Date	<i>N</i>	Source	Method
HD 179 821	1989 May–May	4	Parthasarathy et al. (2005)	Broad-band
	1991 October	1	Trammell et al. (1994)	Spectropolarimetry
	1993 August	1	HPOL data base, Johnson (private communication)	Spectropolarimetry
	1997 June–1998 October	30	Melikian et al. (2000)	Broad-band
IRC +10 420	1976 May–June	1	Craine et al. (1976)	Broad-band
	1989 May	1	Johnson & Jones (1991)	Broad-band
	1991 October	1	Jones et al. (1993)	Broad-band
	1991 October	1	Trammell et al. (1994)	Spectropolarimetry

**Table 4.** A summary of recent photometric observations of IRC +10 420 and HD 179 821. In the fourth column, we give the number of observations taken in each passband, respectively. For IRC +10 420, this acts as an update to the previous tables compiled by Jones et al. (1993) and Oudmaijer et al. (1996).

Object	Date	Band	<i>N</i>	Source
HD 179 821	1988 March to April	<i>V, J, K</i>	1, 2	Hrivnak et al. (1989)
	1990 May–1999 October	<i>V</i>	169	Arhipova et al. (2001)
	1990 May–2005 November	<i>V</i>	254	ASAS catalogue
	1992 June	<i>J, K</i>	1	Kastner & Weintraub (1995)
	1998 October	<i>J, K</i>	1	2MASS data base
IRC +10 420	1996 May–1996 June	<i>J, K</i>	2, 2	Humphreys et al. (1997)
	2001 April	<i>J, K</i>	4, 5	Kimeswenger et al. (2004)
	2002 April–2004 October	<i>V</i>	104	ASAS catalogue

double-peaked and variable emission-line profile. In 2003, the red peak is stronger than the blue peak, but in 2004 the blue peak has become the stronger, while the central absorption component of the double-peaked line has become deeper. Comparison with published data reveals that the red peak is very strong in the present spectrum. Oudmaijer (1998) shows data taken in 1993 of the object, where the blue peak is two to three times stronger than the red one. The EW of the line was  $-25 \text{ \AA}$ , about half that observed now. This evolving blue-to-red peak ratio was also noted by Klochkova et al. (2002).

The spectropolarimetric data show large polarization changes across the line. In each case, this line effect consists of a depolarization over the central part of the line coupled with a rotation to larger angles. The associated  $Q - U$  plots (Fig. 1) also clearly show the line effects. The cluster of data points in the lower right-hand corners of the graphs is due to the stellar continuum, while the excursions to the upper left-hand corners trace the polarization over the H $\alpha$  line. At first glance, the excursions might seem to suggest the presence of structure. However, given that the binning is at the 0.1 and 0.3 per cent level, respectively, and that the ‘structure’ is mostly due to single points offset by less than  $3\sigma$  from the global trends, we proceed under the assumption that the excursions are linear. The intrinsic polarization angle for IRC +10 420 is measured by the excursion from the line centre (which has a lower contribution by the polarization due to electron scattering) to the continuum. Using equation (2), this is  $158^\circ$ , with an estimated error of  $2^\circ$ , and it does not seem to change with time. The magnitude of the excursion gives an indication of the strength of the polarization change and is

similar in 2002 and 2003, but almost twice as large in 2004. Strictly speaking the length of the vector represents a lower limit to the real depolarization because a finite spectral resolution can wash out the line effect. However, the 2002, lower resolution data have a depolarization vector of similar length to the higher resolution, 2003 data. It is therefore plausible that the depolarization (and thus the polarization of the continuum due to electron scattering) is significantly stronger in the 2004 data.

The continuum polarization towards IRC +10 420 consists of three components. First, there is ISP due to dichroic absorption of interstellar dust. This is constant with time and is constant over a small part of the spectrum. In data such as in Fig. 1, this would add a constant vector to the intrinsic  $Q, U$  spectrum. Importantly, the shape of the  $Q, U$  behaviour is not affected by the ISP. Secondly, some polarization may be due to scattered light reflected off circumstellar dust grains. The presence of scattered light is revealed by Kastner & Weintraub (1995) who show that the polarization is significant at large distances from the star. Later, *Hubble Space Telescope* (*HST*) images show substantial extended emission in blue light which is interpreted as scattered light as well (Humphreys et al. 1997, 2002; see also Davies, Oudmaijer & Sahu 2007). When obtaining spatially unresolved data, such as here, any net polarization is due to the asymmetry of the scattering material on the sky. Thirdly, the continuum light can be scattered off free electrons that are very close to the star. Here, imaging polarimetry cannot achieve the spatial resolution required to study the electron-scattering region. The line effect, however, readily reveals its presence.

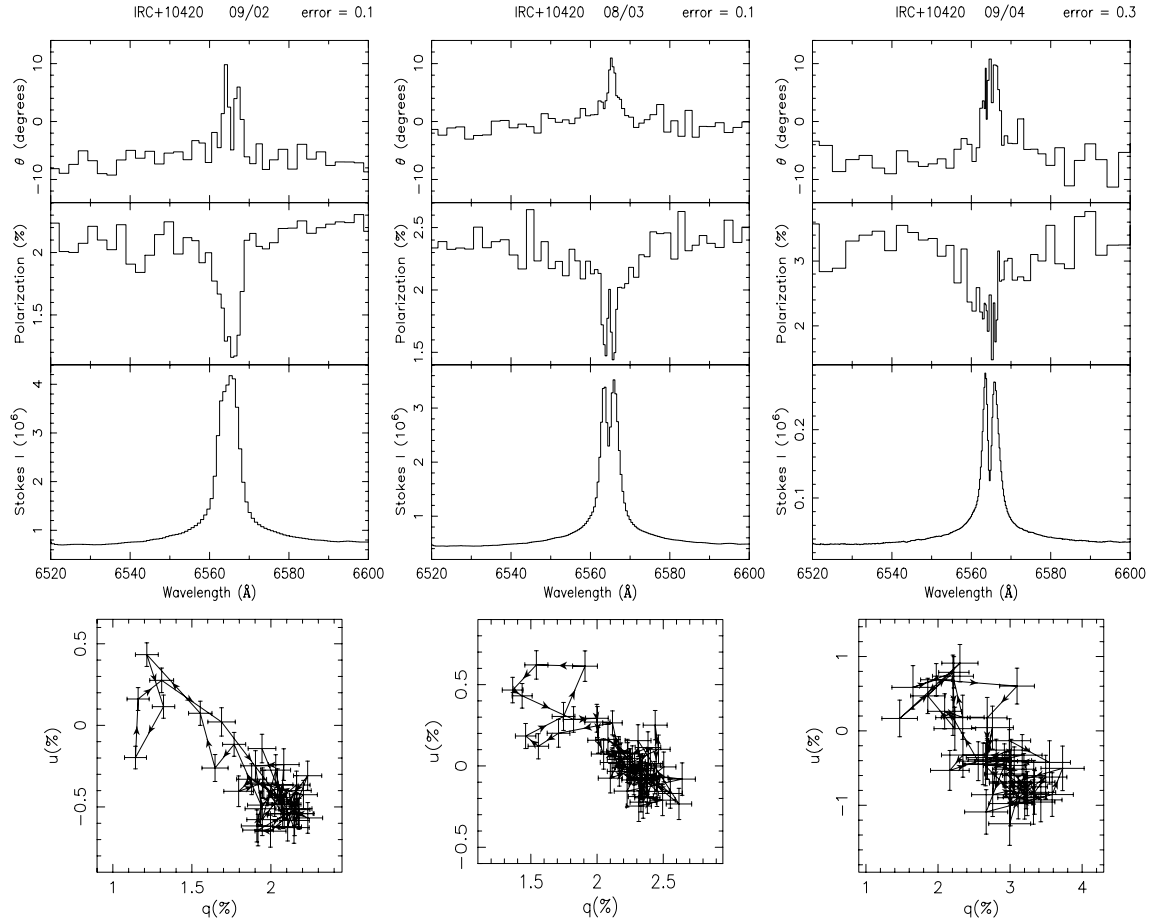


**Figure 1.** Spectropolarimetry of IRC +10420 around H $\alpha$  at different epochs. The upper diagrams are ‘triplets’ of the spectropolarimetric data, which were taken one year apart from one another. The bottom panel of the triplet presents the direct intensity spectrum, the data normally obtained from spectroscopy. The middle panel shows the polarization measured as a function of wavelength. The upper panel shows the corresponding polarization angle. The data are adaptively binned such that each bin has the same observational error derived from Poisson statistics. Here, we have chosen errors of 0.1, 0.1 and 0.3 per cent, respectively, for the 2002, 2003 and 2004 data. Below the triplets, the Stokes  $Q$ ,  $U$  vectors are plotted against each other, and binned to the same precision as the spectra. Depolarization around H $\alpha$  is seen each time and the associated excursions in  $Q - U$  space all point in the same direction.

### 3.1.2 Long-term photo-polarimetry

Our new data are combined with literature data and are shown in Fig. 2. Over the past 30 yr, both the polarization and the angle have increased. To illustrate this, the  $Q$  and  $U$  Stokes vectors are also plotted. The Stokes  $Q$  parameter increases by about 2 per cent, while the  $U$  vector essentially remains constant (see also Fig. 3). Here, we note the Trammell, Dinerstein & Goodrich (1994) data. Their data point (3.7 per cent at  $149^\circ$ ) was taken in the same month as the Jones et al. (1993) data which is 2.0 per cent at  $174^\circ$ . The Trammell et al. measurement strongly deviates from the general 30 yr trend in  $P$ ,  $\Theta$  and  $U$ , and are also significantly different from data taken in the same month. We will proceed assuming that the trend of increasing polarization with time reflects the true long-term polarization behaviour of the object, and have a caveat that, perhaps, the evolution is more complex. In Fig. 3, we plot the broad-band Stokes  $Q$  and  $U$  vectors against one another. Jones et al. (1993) derive an interstellar  $R$ -band polarization of 8 per cent towards IRC +10420 – a value that is not inconsistent with the large reddening towards the object. From their figures, we measure their ISP to be  $Q_{R,ISP} \approx 7.5$  per cent,  $U_{R,ISP} \approx 2.7$  per cent. This value is indicated in Fig. 3. Assuming the H $\alpha$  line centre is not polarized due to electron scattering, its net polarization is due to a combination of ISP and scattering off

circumstellar dust. We can thus get a (very) rough estimate of the circumstellar dust polarization by taking the difference between the H $\alpha$  line centre polarization and the ISP value. Our observed line centre polarizations are close each other. Remarkably, the recent H $\alpha$  line polarization values all lie on the vector connecting the ISP with the origin. Their average distance to the ISP value is  $Q = -6.0$  per cent,  $U = -2.2$  per cent, corresponding to a circumstellar dust polarization of  $P = 6.4$  per cent,  $\Theta = 10^\circ$ . The true value may have a larger polarization at a smaller angle, as the polarization in the centre of the line is probably affected by the resolution. Note that an interesting situation has arisen where the circumstellar dust polarization effectively cancels part of the ISP resulting in smaller net polarization values. Using equation (2), we measure an intrinsic polarization angle for the variations of  $6 \pm 2^\circ$ . This is very close to the orientation found for the circumstellar dust polarization described above and pinpoints the changes in circumstellar dust polarization as a likely cause for the observed variations.

The photometric variability has been discussed extensively by Jones et al. (1993) and Oudmaijer et al. (1996). Here, we give an update on the long-term variability (see Table 4). The  $K$ -band data show a steady fading starting in the mid-seventies. This dimming is mimicked by the data in the  $J$  band, which is known to trace the

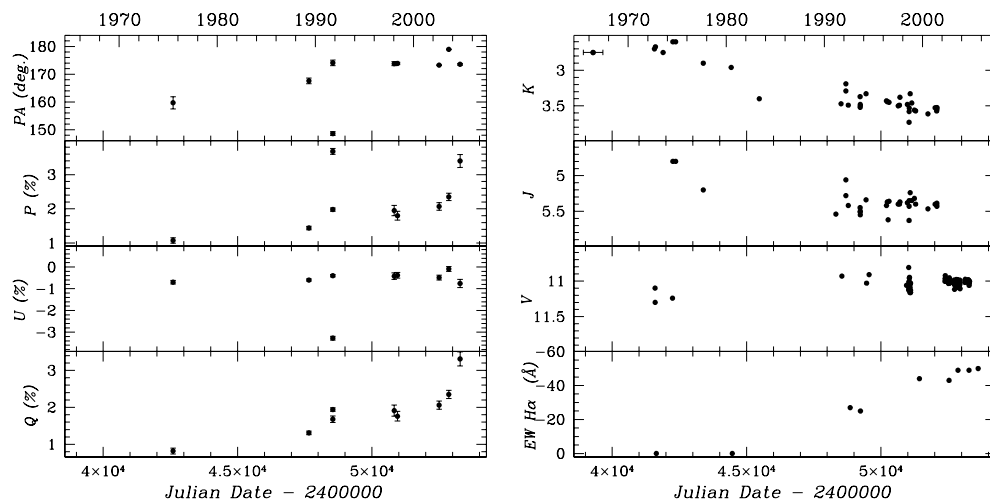


**Figure 2.** Left-hand panel: the polarization and position angle variability of IRC +10420 in the R band. Both the polarization and PA show an increase with time. The bottom two panels show the evolution of the Stokes  $Q$  and  $U$  vectors. Right-hand panel: an updated version from the photometric variations presented in Oudmaijer et al. (1996). The change in the  $J$  band, which traces the stellar photosphere, indicates a temperature increase of the star. Also included is the evolution of the  $H\alpha$  EW which displays a marked strengthening over the years.

stellar photosphere (Oudmaijer et al. 1996). After around 1995, the  $J$ -band magnitudes appear to reach a steady state.

Long-term changes have also been observed in the hydrogen recombination lines. In 1992, Oudmaijer et al. (1994) discovered near-IR recombination emission lines that were previously seen in absorption in 1984. Irvine & Herbig (1986) detected  $H\alpha$  emission in 1986, while previous observations did not show emission. Therefore, the onset of hydrogen recombination emission can be traced to a period between 1984 and 1986 (Oudmaijer et al. 1994). This coincides precisely with a period of strong photometric changes.

EW data of  $H\alpha$  were collected from the literature as well. It is not trivial to obtain these data because of the large width of the line. For example, EW measurements from high-resolution echelle data are not possible as the free spectral range is too small to properly define a baseline and measure the EW accurately. We therefore restrict ourselves to results from spectra with a large free spectral range – essentially no echelle observations. Data are taken from Oudmaijer et al. (1994), Oudmaijer (1998), Humphreys et al. (2002), this paper and Davies et al. (2007), respectively. The results are also shown in Fig. 2.  $H\alpha$  has been increasing in strength, going from upper limits of the EW in the seventies to  $-23 \text{ \AA}$  in the early nineties to  $-50 \text{ \AA}$  in 2005. As the optical brightness has remained constant in that time, these EW changes reflect true line flux changes and imply that more ionized material is present.

## 3.2 HD 179 821

### 3.2.1 Spectropolarimetry

Spectropolarimetric data of HD 179 821 are shown in Fig. 4. No polarization changes are visible across the faint  $H\alpha$  line. The 2002 data have a higher signal-to-noise ratio (SNR), but a weaker  $H\alpha$  emission than in 2004. There are few reports of the  $H\alpha$  line in the literature, but it would appear it is variable in the sense that it varies between weak emission above the continuum (i.e. 10–20 per cent emission above the continuum was observed by Zacs et al. 1996) and weak emission that hardly fills in the underlying absorption as observed here.

The weak emission implies that the number of free scattering electrons is rather limited, which is not inconsistent with the low surface temperature of the star (its spectral type is G4 0-Ia, Keenan & McNeil 1989). Therefore, any continuum polarization due to electron scattering is bound to be low. In such a case, extremely high SNR data are required to reveal a line depolarization, if it were present at all. Alternatively, the hydrogen recombination line emission in HD 179 821 could be due to photospheric shocks. The object has been found to show periodic photometric variations of 140 and 200 d (see Le Coroller et al. 2003). These variations are most likely due to pulsations, and it is common to observe  $H\alpha$  emission due to shocked layers in the photosphere of cool, pulsating stars (e.g. Schmidt et al. 2004 and references therein).

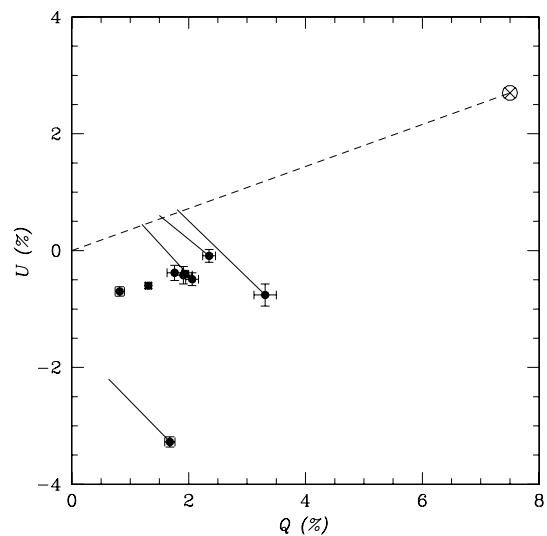


**Figure 3.** A  $Q-U$  diagram of IRC +10420. The  $R$ -band ( $Q, U$ ) data points come from the literature and our new broad-band polarimetry. The dashed line represents the vector towards the ISP, denoted by the crossed circle, as derived by Jones et al. (1993). The continuum values from the spectropolarimetric data are represented by dots and the straight lines show the excursions to the line centre polarization measured from the spectropolarimetry.

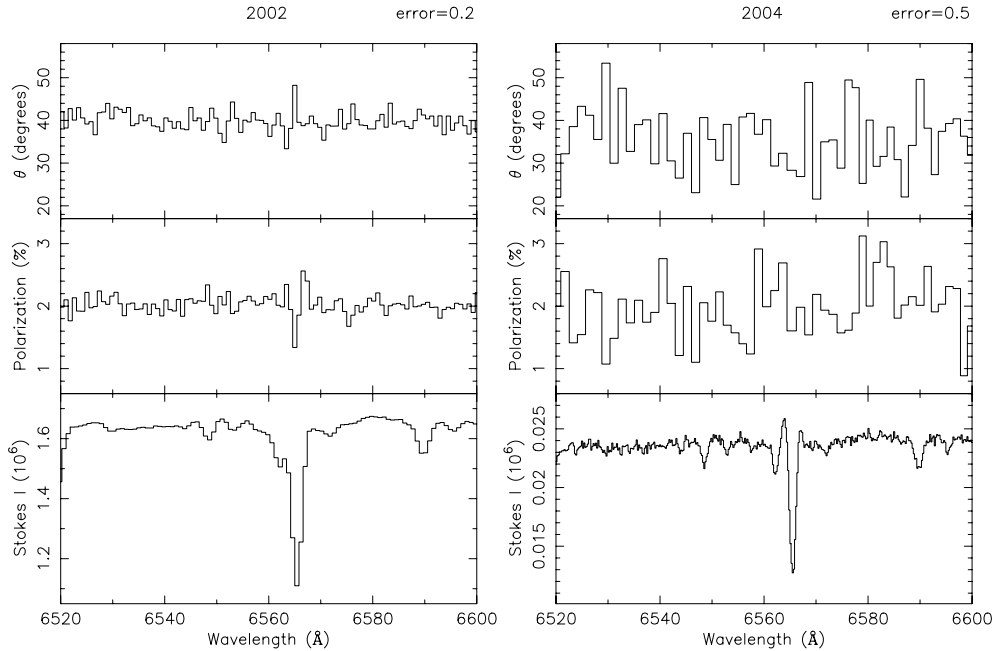


**Figure 4.** As in Fig. 1, but now for HD 179 821 in 2002 (left-hand panel) and 2004 (right-hand panel). The data have been rebinned such that the  $1\sigma$  error in polarization corresponds to the value stated at the top of the triplot, i.e. 0.2 and 0.5 per cent, respectively, as calculated from photon statistics.

### 3.2.2 Long-term photo-polarimetry

The photometry and polarimetry from this paper and the literature of HD 179 821 are plotted in Fig. 5. The longer term optical variability is discussed by Arkhipova et al. (2001). From 1989 to about 1999, the star became fainter by about 0.1 mag, and then returned to its original magnitude. Arkhipova et al. (2001) suggest the photometry may be cyclic on long time-scales. They also find that the object is bluer in  $U - B$  when the star is brightest in  $V$ , which they attribute to pulsations. This is confirmed by the detailed study on shorter term variations in the  $V$  band presented by Le Coroller et al. (2003), which are due to pulsations with periods of the order of hundreds of days. Here, we report the hitherto unnoticed large change in the  $J$  and  $K$  bands. These became fainter by around 0.4 mag in the period 1988–2000.

Fig. 5 shows that HD 179 821 experiences polarization changes (the star is even observed to exhibit no polarization at all for four consecutive days in 1997 November) suggesting that the star is intrinsically polarized. The polarization varies more or less randomly between 0 and 2.5 per cent over the past 15 yr, but we can identify two clear values for the PA, a low value around  $40^\circ$  and a high value of around  $120^\circ$ . When plotting these data in  $QU$  space (Fig. 6), we can see that the data points are distributed around what we can loosely describe as a straight line through the origin.

The move through the origin of the  $QU$  diagram is responsible for the large change in observed polarization angle. This must have happened at least five times: the first occurred between the 1989–1991 Parthasarathy, Jain & Sarkar (2005) data set ( $PA = 40^\circ$ ) and the 1991 Trammell et al. (1994) data point ( $PA = 120^\circ$ ) taken half a year later, when the object moved from the upper half to the lower half in the  $QU$  diagram. After this, a move occurred between 1991 and the HPOL data taken in 1993 (Johnson, private communication; using HPOL, Wolff, Nordsieck & Nook 1996). The object returned back to the lower half as observed by Melikian et al. (2000), who also directly detected such an excursion in 1997–1998 (the non-detections which lie, by definition, at the origin). Finally, a crossing

happened after their observing run, but before our present data was taken. The move through the origin does not necessarily reflect a real  $90^\circ$  rotation, as the ISP may contribute significantly to the total  $Q$ ,  $U$  vectors observed towards the object.

It is hard to determine the ISP towards any object, but we can make an educated guess. Since  $A_V \sim 2$  for HD 179 821 (Hrivnak, Kwok & Volk 1989) and one typically finds that the percentage polarization is equal to the extinction in magnitudes (e.g. Oudmaijer et al. 2001), we can expect an ISP of up to 2 per cent towards the object. A value for the ISP angle may be estimated from the polarization of surrounding field stars. To this end we investigated the compilation of polarized stars due to Heiles (2000). The local ISP appears very ordered towards this part of the sky. We selected all objects with a polarization measurement larger than 0 per cent and within a radius of  $5^\circ$  from the position of HD 179 821. These 22 objects have an average polarization angle of  $50^\circ$  with a scatter of  $24^\circ$ . The catalogue also lists the photometric distances, and the average angle is the same for the 11 furthest ( $>500$  pc) objects. Whatever the magnitude of the polarization, these values indicate that the ISP can be located in the top quadrants of Fig. 6. When taking these angles at face value, and assuming the ISP is oriented in the same direction at large distances as locally, then the ISP towards HD 179 821 is  $50^\circ$  at 2 per cent. This is close to the present-day value of HD 179 821, and, if true, would suggest that HD 179 821 is presently in a relatively quiescent state, yet the polarization is still variable by up to a few per cent. The instances when the object occupies the bottom of the  $QU$  diagram can then be identified as periods where the polarization of HD 179 821 is particularly strong. The optical photometry does not signal any such activity however, and continues its gradual decline to fainter magnitudes.

In short, during the last 15 yr, the observed polarization of HD 179 821 crossed the origin in the  $QU$ -diagram several times. The changes occur along a straight line and suggest some preferred orientation, for which we derive a very rough estimate for the intrinsic angle of  $38^\circ$ . In addition, the polarization changes by 4–5 per cent, while only modest changes in the optical photometry of less than

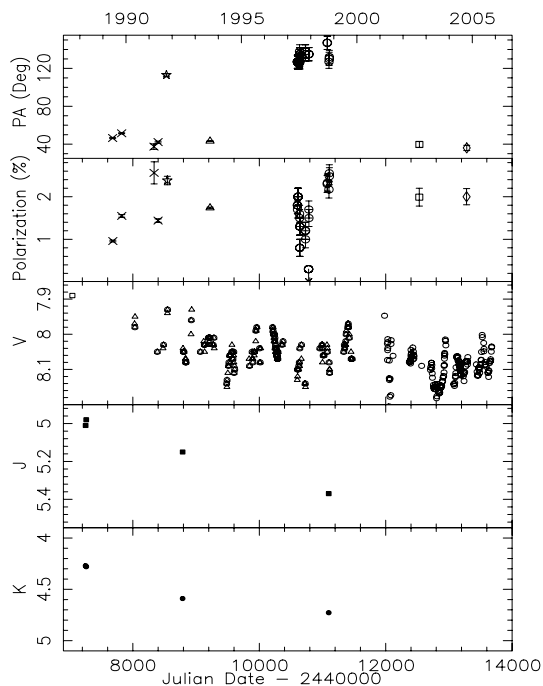


**Figure 5.** The variability of HD 179 821 with time. Plotted is the V-band photometry provided by Hrivnak et al. (1989) (squares), Arkhipova et al. (2001) (triangles) and the All Sky Automated Survey (ASAS) catalogue (Pojmanski, 2002) (circles). The error associated with the photometry measurements provided by Arkhipova et al. is 0.005 mag and those from the ASAS catalogue are less than 0.06 mag. Plotted in the upper two plots are PA and polarization data taken from Parthasarathy et al. (2005) (crosses), HPOL data base (triangle), Trammell et al. (1994) (star), Melikian et al. (2000) (circles) and data presented in this paper from 2002 (squares) and 2004 (rhombi). The PA exhibits large rotations over a 15-yr period, while the polarization indicates the presence of short-term variability. The lower panels show that HD 179 821 has become fainter in *J* and *K*.

0.2 mag occur. Near-IR photometry is sparse, and indicates a gradual faintening of the star. The most recent data point obtained on 1998 October 12, which was a few weeks before the end of Melikian et al. (2000)’s campaign, i.e. when HD 179 821 was, if the ISP value is correct, still in a high state of polarization.

## 4 DISCUSSION

We have observed the only two post-red supergiants with large IR excesses using multi-epoch spectropolarimetry and supplemented these data with long-term photo-polarimetry. We find some striking similarities between the two objects, but also large differences. We will start with the latter.

### 4.1 The ionized gas

The spectropolarimetry reveals a strong line effect in the data of IRC +10 420, but none for HD 179 821. The latter displays weak  $H\alpha$  emission and is much cooler than IRC +10 420. It is therefore not surrounded by much ionized material. As electron scattering is the prime mechanism to produce line effects, it can then be easily understood why there is no line effect towards HD 179 821.

As described earlier, the intrinsic polarization angle due to electron scattering for IRC +10 420 is measured by the excursion from the line centre, and is  $158^\circ$ . This angle remained constant within the

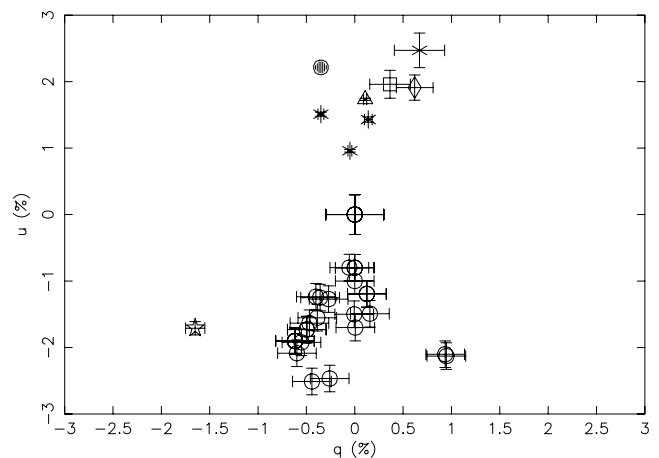


**Figure 6.** A  $Q-U$  diagram of HD 179 821. Each point corresponds to the wavelength-averaged *R*-band continuum values of  $Q$  and  $U$  taken at different epochs. There are groupings of points in two separate areas of the plot, one corresponding to low PA angles (top panel) and the other to high angles (bottom panel). The filled circle shows the position of the ISP (see the text). The other symbols are as in the previous figure.

errorbars during our three observing epochs, whereas the observed polarization increased by 1.5 per cent. Since the excursion across the line in  $QU$  space became larger between 2003 and 2004, we can attribute this increase in continuum polarization to more scatterings of continuum photons by free electrons rather than dust particles.

The presence of the line effect is strong evidence that the electron-scattering region has a geometry that deviates from spherical symmetry. The constant intrinsic polarization angle indicates that the structure has remained stable. The nature of the  $H\alpha$  emitting region, and especially its geometry, has been the topic of much debate, often centring on the question whether it is spherical or not (see the review of the literature by Davies et al. 2007). Davies et al. (2007) use integral field spectroscopy to study reflected light off circumstellar dust of the emission line and show that the  $H\alpha$  line emitting region is not spherically symmetric. Here, we confirm this result.

It is unclear, however, what the polarization angle corresponds to. Assuming that the scattering is optically thin, the structure responsible for the scattering is oriented perpendicular to this at an angle of  $68^\circ$ . A comparison with the larger scale structure observed in *HST* data, which traces the reflection nebosity (Humphreys et al. 1997, 2002) is inconclusive. The angle does not correspond straightforwardly with either the long or short axis. The Hubble data reveal very clumpy structures at subarcsec scales and it proves impossible to link the even smaller scales probed by the electron scattering, with the clumps or larger scale structures in the imaging.

Finally, the increased ionization in IRC +10 420 may be either explained by an increase of mass close to the star, due to either an infall or outflow or due to an increase in temperature.

### 4.2 Temperature evolution

The photometry shows some remarkable similarities between the two objects. Both stars have been subject to studies of their spectral energy distribution (SED, Oudmaijer et al. 1996 and Hrivnak et al. 1989 for IRC +10 420 and HD 179 821, respectively). From fits to their SEDs, it is clear that the near-IR *J*-band photometry samples their photospheres and not the hot dust. In both cases, this *J*-band

magnitude has become fainter over the past few decades. At the same time, their  $V$ -band magnitudes varied only weakly, if at all.

The photometric changes in  $J$ , in particular, the decrease in  $V - J$ , can be explained as being due to bolometric correction effects associated with an increase in stellar temperature. For IRC +10420, this is consistent with published spectra (see Klochkova, Chentsov & Panchuk 1997; Oudmajer 1998). This trend is less obvious more recently. It is likely that the  $J$ -band magnitude has reached a plateau, but it is not apparent whether this implies that the temperature increase has halted or not. The  $V - J$  colour is not very sensitive to changes in spectral type earlier than A0, so an ongoing temperature increase is not ruled out based on the photometry.

$J$ -band data of HD 179821 are much more sparse, but the trend is clear. The object has become fainter in  $J$ . If the change in  $V - J$  colour is due to the changes in effective temperature, then the star has become hotter during this period, in the same way as for IRC +10420. For  $A_V = 2$  (Hrivnak et al. 1989), and combining the intrinsic optical colours for supergiants as provided by Straizys & Kuriliene (1981) and intrinsic near-IR colours due to Koornneef (1983), we find that the star must have evolved to an earlier spectral type by about one or two spectral subtypes.

There is some ambiguity concerning the star's temperature as derived from chemical abundance modelling. For example, Thévenin et al. (2000) favour a lower temperature, consistent with the  $G$  spectral type. This is 1000 K less than Reddy & Hrivnak (1999) and Zacs et al. (1996) determinations using data taken earlier. Thus, it is hard to draw any conclusions on the evolution of the stellar temperature. The near-IR photometric changes may be seen as independent evidence that the star appears to have been evolving towards higher temperatures. Alternatively, the temperature changes may be due to the formation of a pseudo-photosphere (Smith, Vink & de Koter 2004).

The main finding in this section is that both objects appear to be evolving towards the blue in the HR diagram on human time-scales. Judging from the plateauing of the  $J$ -band photometry, IRC +10420 may have slowed down its temperature evolution, or even halted altogether. It has been proposed that the object is hitting the yellow void (de Jager 1998; de Jager et al. 2001; Humphreys et al. 2002) and/or the red-edge of the bistability zone (Smith et al. 2004). In this case, further evolution is prevented unless a large part of its (pseudo-)photosphere is shredded. It will be interesting to follow the object to see whether a large outburst indeed will happen.

### 4.3 Polarization changes

A further similarity between the two objects is the significant polarization variability over the past decades. IRC +10420 increased its polarization (as seen in the  $QU$  diagram, Fig. 3) by about 2.5 per cent. HD 179821's polarization changed by more than 5 per cent, following a straight line in  $QU$  space (Fig. 6). Such changes are not uncommon in stellar objects, for example, UX Ori variables and some T Tauri stars (see e.g. Grinin 1994; Oudmajer et al. 2001). For these objects, rotating clumpy circumstellar discs can result in large polarization changes. These occur when the clumps move into the line of sight of the objects, reducing the optical brightness, often considerably by many magnitudes, and thereby increasing the contribution of polarized light. However, here, in the case of both objects, the changes are not accompanied by large changes in the optical photometry. To make matters worse, a direct consequence of the UX Ori scenario, to explain the strong polarization variations, is that the obscuring dust is located close to the star in a compact, hot structure (Dullemond et al. 2003). This means that

a strong near-IR excess should be present and readily observable. IRC +10420 shows evidence for a significant near-IR excess due to hot dust. In contrast, the near-IR photometry of HD 179821 does not show any sign of hot dust close to the star and is best explained by photospheric emission (Hrivnak et al. 1989).

#### 4.3.1 The electron and dust scattering of IRC +10420

The, variable, continuum polarization of IRC +10420 is due to a combination of dust and electron scattering. The intrinsic PA ( $10^\circ$ ) of the circumstellar dust polarization was derived earlier from the vector connecting the ISP and the line centres of the  $H\alpha$  emission. This PA corresponds to the short axis observed in the larger scale nebulosity of IRC +10420 and may signify a circumstellar dusty disc structure. The intrinsic angle of the electron-scattering region is  $158^\circ$  and is not easily identified with the larger scale structures observed in the *HST* images. In the last observing epoch, 2004, the line depolarization vector was much stronger than previously observed. Although resolution effects may have affected the amplitude of the excursion, the much larger continuum polarization in 2004 indicates that enhanced electron scattering is responsible for the most recent increase in polarization. This is supported by the fact that the continuum polarization moved along the line vector in the  $QU$  diagram (Fig. 3) as well. The PA measured for the  $QU$  vector between the two recent most dates is  $166 \pm 3^\circ$ , very close to the line polarization vectors. Such an increase is not inconsistent with the fact that the  $H\alpha$  emission EW hardly changed. Polarization due to (optically thin) electron scattering is more sensitive than (optically thick)  $H\alpha$  emission for tracing ionized material (see e.g. Bjorkman & Meade 2005).

How does this compare to the longer term changes? The polarization evolves along a more or less straight line with a slope corresponding to a PA of  $6 \pm 2^\circ$ , which closely corresponds to the intrinsic PA of the dust scattering material. If the ISP determined value by Jones et al. (1993) is correct, then it is fair to assume that a decreasing circumstellar dust polarization is the main contributor to the long-term variability. A probable cause for this is a clearing dust shell. This can be tested by producing SED model fits to photometric data taken at several epochs.

In summary, by combining the intrinsic PA of both dust and electron scattering and using the ISP, a relatively simple picture seems to emerge from the variability of the polarization of IRC +10420. At first, a clearing dust shell dominates the polarization behaviour, followed by a significant increase of polarization due to electron scattering. The larger electron scattering is consistent with the observed increase in  $H\alpha$  emission, while the dust clearing can be tested with modelling the circumstellar dust.

This global picture is probably not the final answer however. Even the data discussed here present more questions already. For example, it is not clear why the point taken by Trammell et al. in 1991 strongly deviates from all other values (even one taken in the same month). The  $H\alpha$  depolarization they observe is consistent with what we find 10 yr later, and confirms that part of the polarization is due to electron scattering. The large continuum value would indicate a violent event that led to a polarization increase of several per cent within weeks; however, there is no other evidence to suggest such sudden changes in other observations of IRC +10420. Similarly, it is not obvious why the onset of  $H\alpha$  line emission in the early nineties, and its corresponding polarization of 1–1.5 per cent, is not detected in the long-term polarimetry, which follows a more or less straight line from the seventies to the current data. A speculation is

that a varying, rotating component of electron scattering was present from the onset. Given the increase in H $\alpha$  emission, it is possible that the electron scattering has become more optically thick. If part of the photons scatter more than once in their escape from the electron-scattering region, a full or partial flip in the position angle can result (see e.g. Vink et al. 2005).

#### 4.3.2 *But what about HD 179 821?*

The changes observed for HD 179 821 are less straightforward to interpret. The major question is how large changes over such an extended period can occur while, apart from the polarization, other observations of the star show mild variability at best. First, we note that the ISP is hardly likely to vary on human time-scales. This is supported by the results from a survey of polarization standard stars which reveals no variability in the observed polarization down to extremely low levels (Clarke & Naghizadeh-Khouei 1994). The H $\alpha$  emission is insufficiently strong to suggest the presence of a large electron-scattering region, let alone one that it is variable enough to explain the observed polarization changes. Below we discuss the several possibilities that can account for the polarization and its variability observed towards HD 179 821.

**4.3.2.1 *Asymmetric circumstellar material.*** Having been forced to rule out electron scattering as being responsible for the variability, we now consider scattering by circumstellar dust. The presence of dust scattering was shown in the imaging polarimetry by Kastner & Weintraub (1995). The fact that our, unresolved, data show a net polarization would normally indicate that part of the scattering geometry deviates from spherical symmetry. However, this is not supported by existing imaging data of the circumstellar material of the object. The scattering dust traced by Kastner & Weintraub (1995) stretches over several arcsec, but appears to be distributed spherically symmetrically. *HST* images published by Ueta, Meixner & Bobrowsky (2000) show small-scale structure but largely a round appearance. The CO rotational data maps by Bujarrabal, Alcolea & Planesas (1992) show a slightly elongated structure at larger ( $\sim 5$  arcsec) distances from the star at a PA of  $50^\circ$ .

Even if the slight asymmetry would be responsible for the observed net polarization, it is hard to reconcile this with the observed variability. With a kinematic age of the order of thousands of years (e.g. Kastner & Weintraub 1995), one would not expect changes at a fraction of this period, i.e. 15 yr, to still be traceable. A more practical objection to the extended emission being variable is that the intensity of the scattered light rapidly drops as a function of distance to the star, so there is simply not enough light available to induce variations of 4 per cent in polarization in the total light.

A final possibility is that a compact asymmetric structure much closer to the star is responsible for the variable polarization. As mentioned earlier, the SED of the object leaves no room for a significant, hot dusty component. A caveat is, of course, that the near-IR photometry of the object is limited, so any sudden, short-lived events could have been easily missed. If the ISP value is, as the data suggest, in the upper half of the *QU* diagram, the major polarization activity occurs when the object occupies the lower half of the *QU* diagram. A prediction would then be that during such periods, excess radiation in the near-IR due to hot dust would be present. Near-IR data of HD 179 821 is very sparse, but the last set of *J*, *K* photometry from the Two-Micron All-Sky Survey (2MASS) was taken during Melikian's observing period. These data follow the gradual faintening of the star in the near-IR and do not indicate any excess emission. In addition, the optical photometry appears steady throughout.

For completeness, we do note that Oudmaijer et al. (1995) found variable first-overtone CO emission at 2.3  $\mu$ m towards this object. This emission typically arises in hot, dense material within the dust sublimation radius. Oudmaijer et al. interpreted this as variable mass loss. If the CO emission originates from a geometry that is not spherically symmetric, it could be associated with ejections of dense gas similar to, but shorter than, for example, the asymmetric mass-loss event observed towards HD 45 677 (Patel et al. 2006). The resulting situation could give rise to Rayleigh scattering and a net polarization of light. However, whether this would give rise to the large polarization variations is not clear. We do point out that CO emission from the yellow hypergiant  $\rho$  Cas could also be explained by shocks due to pulsations in the stellar photosphere (Gorlova et al. 2006). This brings us to the central star as the origin of the variations.

**4.3.2.2 *An asymmetric star illuminating the dust shell.*** Above, we considered the case of a central source surrounded by asymmetric scattering media. The asymmetries involved result in a net polarization of the total light. However, we tacitly assumed the central object to be either a point source or an isotropically emitting sphere.

It is well known that when a central source illuminates a spherically symmetric envelope, any asymmetries in the *central source* can induce a net polarization, as, for example, reviewed by Boyle et al. (1986), who find that a photosphere with a non-uniform surface brightness can result in net polarization when its radiation is scattered off circumstellar dust. Other examples of change are found in the polarization spectra of evolved stars where it has been inferred that different molecular bands cover different parts of the stellar photosphere (Biegging et al. 2006). The polarization changes over molecular bands can be explained by both Rayleigh scattering by particles in clouds high in the atmosphere and scattering due to circumstellar dust (Raveendran 1991). In all these cases, the break from symmetry is not due to the circumstellar material, but due to the asymmetric illuminating source.

The extensive photometric observations and period analysis of Le Coroller et al. (2003) indicate that HD 179 821 is a non-radial pulsator (NRP). It is not yet clear whether the shape of the star changes altogether, as we lack the spectral data (Le Coroller et al. quote unpublished data implying that the velocity variations are modest), or due to changes in surface temperature, the situation Le Coroller et al. prefer. In either case, the circumstellar material will be irradiated by an asymmetric source. Then, the polarization changes can be expected to occur around a preferred axis, as, apart from rotation, the pulsation nodes are not expected to stochastically change position on the star.

In order to investigate whether it is plausible that a star with an aspherical shape can yield observable polarization, we performed some test calculations of a star covered by large spots, surrounded by a spherically symmetric dust shell. The model set-up consists of a star with a spot. In the situation where one (bright) spot is present, the polarization will increase with viewing angle. That is to say, if the spot is located in the line of sight, we will see its light directly and not much net polarization will be measured. If on the other hand the system is inclined, less direct light will be seen and the polarized light contribution increases, hence a larger polarization is observed. We should also note that unless the scattering occurs very close to the star (at a few stellar radii), the polarization percentage is independent on the radius of the shell. This is due to the constant geometry of the situation.

For the simple case, where all the stellar flux is radiated from one spot covering 10 per cent of the stellar surface, we find that polarizations up to 3 per cent are readily produced when the star is mildly

inclined. For smaller surface areas, the polarization can be even larger, exceeding 10 per cent. This result confirms earlier studies which used less extreme parameters (Raveendran 1991; Al-Malki et al. 1999). Of course, this is an idealized situation, but it demonstrates that net polarizations of the order of per cent are certainly possible. Indeed, from an observational point of view, polarization changes of around 1 per cent have been observed towards Betelgeuse (Hayes 1984). These changes were due to variable hotspots on the stellar surface. Therefore, polarization changes can indeed be of the order of few per cent if the star itself is anisotropic.

One could argue why the polarization variability is not modulated by the 140- or 200-d period. Perhaps it is on the shorter term, but we lack the data to properly investigate this. However, where we could match photometric and polarimetric data, on shorter time-scales it appears that the polarization values closely follow the photometry. It is therefore possible that the polarization is variable at similar time-scales to the pulsations. A further question is why such long-term changes are observed. We note that the mean photometry shows long-term changes, probably tracing the global evolution of the photosphere, which would have an effect on the non-radial pulsations. Significantly, the preferred plane would not necessarily change, and this is found.

A critical test of the scenarios discussed above is simultaneous photo-polarimetric monitoring of HD 179 821. If non-radial pulsations are responsible for the observed polarization, both observables should be strongly correlated. If, on the other hand, episodic mass ejections are the main cause of the variations, we would expect enhanced near-IR emission due to hot dust during significant polarization changes.

## 5 CONCLUSION

We have presented spectropolarimetry and long-term photopolarimetry for two post-red supergiants. A strong depolarization across the  $H\alpha$  emission line is found for IRC +10420, suggesting an electron-scattering region that is not circularly symmetric, confirming the results of Davies et al. (2007), who found such evidence from their integral field spectroscopy of the object. The time evolution indicates that the source has increased in temperature until at least 1995, after which the  $J$ -band photometry indicates this may have levelled off. If the temperature increase of the object has indeed halted, an increase in mass-loss or mass-infall rate can be responsible for the observed  $H\alpha$  emission and polarization.

HD 179 821, a cooler object, has less  $H\alpha$  emission, and no depolarization across the  $H\alpha$  line could be detected. The photometry implies that this evolved object is also undergoing a change in temperature. Hitherto, temperature determinations of the object were inconclusive, but if the star is a G supergiant, then the observed change in photometry suggests it has become earlier by one or two subclasses. Strong changes at the 5 per cent level in polarization over the past 15 yr have been detected. During the same time, the optical photometry has only varied by at most 0.2 mag. The most obvious explanations for this observation such as changes in either electron or dust scattering can be ruled out. A complication is that the polarization is not correlated with any other observable. The possibility that the star undergoes irregular, asymmetric, mass ejections is discussed. However, there is a little evidence for the occurrence of such events. Instead, it is proposed that the star itself is asymmetric and that its anisotropic radiation, which is scattered off the circumstellar dust, results in the net polarization observed.

## ACKNOWLEDGMENTS

We wish to thank the referee, Professor Kenneth H. Nordsieck, for his detailed reading of the paper and constructive comments. We thank Willem-Jan de Wit for reading the manuscript. Based on observations conducted on the WHT, the NOT and the CST on the Canary islands, the AAT in Australia and the TSO in Kazakhstan. RDO is grateful for the support from the Leverhulme Trust for awarding a Research Fellowship. JCM and MP acknowledge PhD student funding from PPARC/STFC and the University of London, respectively. We are grateful to Joni Johnson for allowing us to use her HPOL data on HD 179 821.

## REFERENCES

- Al-Malki M. B., Simmons J. F. L., Ignace R., Brown J. C., Clarke D., 1999, *A&A*, 347, 919
- Arkipova V. P., Ikonnikova N. P., Noskova R. I., Sokol G. V., Shugarov S. Y., 2001, *Astron. Lett.*, 27, 156
- Bergner Y. K., Bondarenko S. L., Miroshnichenko A. S., Yudin R. V., Yu. Y. N., Moraley Y. D., Schumacher A. V., 1988, *Izvestia Glavn. Astron. Obs. v Pulkove*, 205, 142
- Biegner J. H., Schmidt G. D., Smith P. S., Oppenheimer B. D., 2006, *ApJ*, 639, 1053
- Bjorkman K. S., Meade M. R., 2005, in Adamson A., Aspin C., Davis C. J., Fujiyoshi T., eds, *ASP Conf. Ser. Vol. 343, Astronomical Polarimetry: Current Status and Future Directions*. Astron. Soc. Pac., San Francisco, p. 406
- Boyle R. P., Aspin C., McLean I. S., Coyne G. V., 1986, *A&A*, 164, 310
- Bujarrabal V., Alcolea J., Planesas P., 1992, *A&A*, 257, 701
- Castro-Carrizo A., Quintana-Lacaci G., Bujarrabal V., Neri R., Alcolea J., 2007, *A&A*, 465, 457
- Clarke D., Naghizadeh-Khouei J., 1994, *AJ*, 108, 687
- Craine E. R., Schuster W. J., Tapia S., Vrba F. J., 1976, *ApJ*, 205, 802
- Davies B., Oudmaijer R. D., Vink J. S., 2005, *A&A*, 439, 1107
- Davies B., Oudmaijer R. D., Sahu K. C., 2007, *ApJ*, 671, 2059
- de Jager C., 1998, *A&AR*, 8, 145
- de Jager C., Lobel A., Nieuwenhuijzen H., Stothers R., 2001, *MNRAS*, 327, 452
- de Wit W., Davies B., Oudmaijer R. D., Groenewegen M., Hoare M., Malbet F., 2007, *A&A*, in press (arXiv:0711.4975)
- Dougherty S. M., Taylor A. R., 1992, *Nat*, 359, 808
- Dullemond C. P., van den Ancker M. E., Acke B., van Boekel R., 2003, *ApJ*, 594, L47
- Dwarkadas V. V., Balick B., 1998, *AJ*, 116, 829
- Dwarkadas V. V., Owocki S. P., 2002, *ApJ*, 581, 1337
- Gorlova N., Lobel A., Burgasser A. J., Rieke G. H., Ilyin I., Stauffer J. R., 2006, *ApJ*, 651, 1130
- Grinin V. P., 1994, in P. S., Perez M. R., van den Heuvel E. P. J., eds, *ASP Conf. Series Vol. 62, The Nature and Evolutionary Status of Herbig Ae/Be Stars*. Astron. Soc. Pac., San Francisco, p. 63
- Habing H. J., Tignon J., Tielens A. G. G. M., 1994, *A&A*, 286, 523
- Hayes D. P., 1984, *ApJS*, 55, 179
- Heiles C., 2000, *AJ*, 119, 923
- Hrivnak B. J., Kwok S., Volk K. M., 1989, *ApJ*, 346, 265
- Humphreys R. M., Strecker D. W., Murdock T. L., Low F. J., 1973, *ApJ*, 179, L49
- Humphreys R. M. et al., 1997, *AJ*, 114, 2778
- Humphreys R. M., Davidson K., Smith N., 2002, *AJ*, 124, 1026
- Irvine C. E., Herbig G. H., 1986, *IAU Circ.* 4286, 1
- Johnson J. J., Jones T. J., 1991, *AJ*, 101, 1735
- Jones T. J. et al., 1993, *ApJ*, 411, 323
- Jura M., Velusamy T., Werner M. W., 2001, *ApJ*, 556, 408
- Kastner J. H., Weintraub D. A., 1995, *ApJ*, 452, 833
- Keenan P. C., McNeil R. C., 1989, *ApJS*, 71, 245
- Kerschbaum F., Groenewegen M. A. T., Lazaro C., 2006, *A&A*, 460, 539
- Kimeswenger S., et al., 2004, *A&A*, 413, 1037

- Klochkova V. G., Chentsov E. L., Panchuk V. E., 1997, *MNRAS*, 292, 19
- Klochkova V. G., Yushkin M. V., Chentsov E. L., Panchuk V. E., 2002, *Astron. Rep.*, 46, 139
- Koornneef J., 1983, *A&A*, 128, 84
- Le Coroller H., Lèbre A., Gillet D., Chapellier E., 2003, *A&A*, 400, 613
- Leonard D. C., Li W., Filippenko A. V., Foley R. J., Chornock R., 2005, *ApJ*, 632, 450
- Mazzali P. A. et al., 2003, *ApJ*, 599, L95
- Melikian N. D., Magnan C., Eritsian M. A., Karapetian A. A., 2000, *Astrophys.*, 43, 430
- Mészáros P., 2003, *Nat*, 423, 809
- Nordsieck K. H. et al., 2001, in de Groot M., Sterken C., eds, *ASP Conf. Ser. Vol. 233, P Cygni 2000: 400 Years of Progress*. Astron. Soc. Pac., San Francisco, p. 261
- Oudmaijer R. D., 1998, *A&AS*, 129, 541
- Oudmaijer R. D., 2007, in Hartquist T. W., Falle S. A. E. G., Pittard J. M., eds, *Diffuse Matter From Star Forming Regions to Active Galaxies*. Springer-Verlag, Berlin, p. 83
- Oudmaijer R. D., Drew J. E., 1999, *MNRAS*, 305, 166
- Oudmaijer R. D., Geballe T. R., Waters L. B. F. M., Sahu K. C., 1994, *A&A*, 281, L33
- Oudmaijer R. D., Waters L. B. F. M., van der Veen W. E. C. J., Geballe T. R., 1995, *A&A*, 299, 69
- Oudmaijer R. D., Groenewegen M. A. T., Matthews H. E., Blommaert J. A. D. L., Sahu K. C., 1996, *MNRAS*, 280, 1062
- Oudmaijer R. D., Palacios J., Eiroa C., Davies J. K., de Winter D., Ferlet R. E. A., 2001, *A&AS*, 379, 564
- Oudmaijer R. D., Davies B., de Wit W., Patel M., 2008, in D. Luttermoser B., Smith R. S., eds, *ASP Conf. Ser., Biggest, Baddest, Coolest Stars*. Astron. Soc. Pac., San Francisco, preprint (arXiv:0810.2315)
- Parthasarathy M., Jain S. K., Sarkar G., 2005, *AJ*, 129, 2451
- Patel M., Oudmaijer R. D., Vink J. S., Mottram J. C., Davies B., 2006, *MNRAS*, 373, 1641
- Poeckert R., 1975, *ApJ*, 196, 777
- Poeckert R., Marlborough J. M., 1976, *ApJ*, 206, 182
- Quirrenbach A. et al., 1997, *ApJ*, 479, 477
- Raveendran A. V., 1991, *A&A*, 243, 445
- Reddy B. E., Hrivnak B. J., 1999, *AJ*, 117, 1834
- Schmidt E. G., Johnston D., Lee K. M., Langan S., Newman P. R., Snedden S. A., 2004, *AJ*, 128, 2988
- Slowik D. J., Peterson D. M., 1995, *AJ*, 109, 2193
- Smith N., Vink J. S., de Koter A., 2004, *ApJ*, 615, 475
- Straizys V., Kuriliene G., 1981, *Ap&SS*, 80, 353
- Thévenin F., Parthasarathy M., Jasniewicz G., 2000, *A&A*, 359, 138
- Trammell S. R., Dinerstein H. L., Goodrich R. W., 1994, *AJ*, 108, 984
- Ueta T., Meixner M., Bobrowsky M., 2000, *ApJ*, 528, 861
- Vink J. S., Drew J. E., Harries T. J., Oudmaijer R. D., 2002, *MNRAS*, 337, 356
- Vink J. S., Drew J. E., Harries T. J., Oudmaijer R. D., Unruh Y., 2005, *MNRAS*, 359, 1049
- Wang L., Baade D., Höflich P., Wheeler J. C., 2003, *ApJ*, 592, 457
- Weis K., 2003, *A&A*, 408, 205
- Wolff M. J., Nordsieck K. H., Nook M. A., 1996, *AJ*, 111, 856
- Wood K., Bjorkman K. S., Bjorkman J. E., 1997, *ApJ*, 477, 926
- Zacs L., Klochkova V. G., Panchuk V. E., Spelmanis R., 1996, *MNRAS*, 282, 1171

This paper has been typeset from a  $\text{\TeX}/\text{\LaTeX}$  file prepared by the author.